JACC: ASIA VOL. 4, NO. 12, 2024

ORIGINAL RESEARCH

Right Ventricular Restrictive Physiology Is Associated With Right Ventricular Direct Flow From 4D Flow CMR

Xiaodan Zhao, PhD,[a,*] Phong Teck Lee, MBChB,[a,*] Liwei Hu, MSc,[b] Ru-San Tan, MBBS,[a,c] Ping Chai, MBBS, MMED,[d,e] Tee Joo Yeo, MBBS, MMED,[d,e] Shuang Leng, PhD,[a,c] RongZhen Ouyang, MD, PhD,[b] Jennifer Ann Bryant, PhD,[a,c] Lynette L.S. Teo, MBChB, MMED,[d,e] Rob J. van der Geest, PhD,[f] James W. Yip, MBBS,[d,e] Ju Le Tan, MBBS,[a,c] Yumin Zhong, MD, PhD,[b,†] Liang Zhong, PhD[a,c,g,†]

ABSTRACT

BACKGROUND Right ventricular restrictive physiology (RVRP) is a common occurrence in repaired tetralogy of Fallot (rTOF). The relationship of RVRP with biventricular blood flow components and kinetic energy (KE) from 4-dimensional (4D) flow cardiovascular magnetic resonance (CMR) is unclear.

OBJECTIVES The purpose of this study was to investigate the association of 4D flow CMR parameters with RVRP in rTOF patients.

METHODS A total of 103 rTOF patients and 62 age and sex-matched healthy control subjects were prospectively recruited. All participants underwent CMR (cine, 2-dimensional phase-contrast, and 4D flow sequences), and cardiopulmonary exercise test in adult populations. RVRP was identified from pulmonary artery flow curve using 2-dimensional phase-contrast images. Biventricular flow components (direct flow, retained inflow, delayed ejection flow, and residual volume) and KE parameters normalized to end-diastolic volume (KEi_{EDV}) were analyzed encompassing global, peak systolic, average systolic, average diastolic, peak E-wave, and peak A-wave.

RESULTS Compared with control subjects, rTOF patients had significantly lower RV direct flow and higher RV residual volume (both $P < 0.001$). All RV KEi_{EDV} parameters, except peak A-wave, were higher in rTOF patients. In rTOF patients, 70 of 103 (68%) had RVRP, with increasing RV direct flow (27% vs 20%; $P = 0.002$) and RV peak E-wave KEi_{EDV} (28.4 vs 20.7μJ/mL; $P = 0.015$) and decreasing RV residual volume (37% vs 42%; $P = 0.039$) than rTOF without RVRP. Exercise capacity was impaired in rTOF, although comparable between RVRP subgroups. Multivariable analysis revealed RV direct flow was an independent predictor of RVRP (OR: 1.158; 95% CI: 1.074-1.249; $P < 0.001$).

CONCLUSIONS RVRP is associated with dilated RV, higher pulmonary regurgitation, and higher RV direct flow. (Integrated Computational modeling of Right Heart Mechanics and Blood Flow Dynamics in Congenital Heart Disease; NCT03217240) (JACC Asia. 2024;4:912-924) © 2024 The Authors. Published by Elsevier on behalf of the American College of Cardiology Foundation. This is an open access article under the CC BY-NC-ND license (http://creativecommons.org/licenses/by-nc-nd/4.0/).

From the [a]National Heart Research Institute Singapore, National Heart Centre Singapore, Singapore; [b]Duke-NUS Medical School, Singapore; [c]Department of Radiology, Shanghai Children's Medical Center, Shanghai Jiao Tong University School of Medicine, Shanghai, China; [d]National University Hospital Singapore, Singapore; [e]Yong Loo Lin School of Medicine, National University of Singapore, Singapore; [f]Department of Radiology, Leiden University Medical Center, Leiden, the Netherlands; and the [g]Department of Biomedical Engineering, National University of Singapore, Singapore. *Drs Zhao and Lee contributed equally to this work as first authors. †Drs Yumin Zhong and Liang Zhong contributed equally to this work as corresponding authors.
The authors attest they are in compliance with human studies committees and animal welfare regulations of the authors' institutions and Food and Drug Administration guidelines, including patient consent where appropriate. For more information, visit the Author Center.

Manuscript received March 28, 2024; revised manuscript received August 14, 2024, accepted August 24, 2024.

ISSN 2772-3747 https://doi.org/10.1016/j.jacasi.2024.08.019

Tetralogy of Fallot (TOF) is the most prevalent form of cyanotic congenital heart disease, affecting approximately 0.28 every 1,000 live births, with an equal sex distribution.[1] Advances in diagnostic techniques and postoperative care have enabled individuals born with TOF to undergo corrective surgical repair early in life, leading to their survival into adulthood. Following surgical repair of TOF, a common phenomenon known as right ventricular restrictive physiology (RVRP) emerges. It is characterized by the presence of end-diastolic forward flow in the main pulmonary artery (MPA) during atrial contraction.[1] The postulated pathophysiological cause of RVRP is elevated right ventricular (RV) end-diastolic pressure stemming from increased RV myocardial stiffness and reduced RV compliance.[2] Its incidence varies between 50% to 70% among repaired tetralogy of Fallot (rTOF) patients.[3] However, the impact of RVRP on patients' clinical status remains a topic of debate. Some studies have indicated that RVRP is beneficial in adult rTOF patients. It shortens the duration of pulmonary regurgitation (PR), resulting in reduced pulmonary regurgitant volume and fraction. There is evidence that RVRP resulted in reduced cardiomegaly and improved exercise capacity.[4] However, other studies have found that pediatric patients with RVRP had increased RV volumes and decreased exercise capacity.[5,6] Additionally, other research has shown that RVRP does not significantly affect exercise capacity.[3]

Cardiovascular magnetic resonance (CMR) has demonstrated excellent reproducibility in measuring ventricular volumes and has become the reference standard for quantification of ventricular size and function in rTOF patients. Four-dimensional (4D) flow CMR is a powerful technique that simultaneously quantifies blood flow in 3 orthogonal directions within a defined volume of interest, providing a time-resolved depiction throughout the cardiac cycle, and has shown its superiority than 1-directional velocity-encoded 2-dimensional (2D) phase-contrast (PC) flow. The primary advantage of 4D flow CMR is its ability to allow retrospective placement of analysis planes at any location within the acquisition volume.[7] This flexibility enables comprehensive and detailed assessment of blood flow dynamics throughout the heart and major vessels without the need for repeat scans. In rTOF, 4D flow CMR has been used for the characterization of flow patterns and hemodynamics in terms of abnormal flow organization,[8,9] derangements of ventricular kinetic energy (KE),[9-11] increased turbulent KE in the RV,[12] pathological vortices,[13] increased longitudinal circulation (area integral of vorticity) in the MPA,[14] elevated viscous energy loss in RV outflow tract,[15] and pulmonary artery (PA).[16] A comprehensive systemic review of 4D flow application in rTOF was presented by Elsayed et al.[17] Until now, no study has explored the relationship between 4D flow hemodynamics and RVRP in both pediatric and adult rTOF patients. Hence, in the current study, we aimed to characterize the hemodynamics using biventricular flow components and KE in rTOF and healthy control subjects and investigate their associations with RVRP in rTOF patients.

ABBREVIATIONS AND ACRONYMS

AO = aorta
CHD = congenital heart disease
EDV = end-diastolic volume
ESV = end-systolic volume
KE = kinetic energy
KEi_{EDV} = kinetic energy normalized to end-diastolic volume
LV = left ventricle
MPA = main pulmonary artery
PA = pulmonary artery
PC = phase-contrast
PR = pulmonary regurgitation
rTOF = repaired tetralogy of Fallot
RV = right ventricle

METHODS

STUDY POPULATION. From June 2017 to February 2022, we have established a prospective clinical and image registry of TOF patients with reference control subjects, and registered at ClinicalTrials.gov (NCT03217240). The inclusion criteria of rTOF were as follows: 1) survivors of TOF repair more than 1 year after repair without residual intracardiac shunting, pulmonary stenosis (Doppler gradient >30 mm Hg), supraventricular arrhythmias, and significant ventricular arrhythmias (low grade >2); and 2) age 12 to 80 years. The inclusion criteria for healthy volunteers were as follows: 1) age 12 to 80 years; 2) asymptomatic and ambulant; and 3) resting blood pressure <140/90 mm Hg. The exclusion criteria for all subjects were as follows: 1) contraindication to CMR examination; 2) noncardiac illness with life expectancy of <2 years; 3) previous heart, kidney, liver, or lung transplantation; and 4) pregnancy. Additional exclusion criteria for adult healthy subjects were as follows: 1) history of any major medical problems, cardiovascular disease or cardiovascular risk factor (eg, hypertension, diabetes, or dyslipidemia), or significant renal or lung disease; 2) concurrently taking medications for cardiovascular disease or cardiovascular risk factor (eg, for hypertension); and 3) heavy smoking (over 5 cigarettes/d or who had quit smoking for <12 months and had smoked over 5 cigarettes/d previously). Adult rTOF and control subjects were selected from this study.

Pediatric patients who were scheduled to undergo clinically indicated CMR were prospectively recruited at Shanghai Children's Medical Center between August 2019 and January 2020. Same-day transthoracic echocardiogram (TTE) was also performed. Inclusion criteria for pediatric rTOF were age <18 years and no history of other cardiac surgeries. Exclusion criteria included the presence of palliative shunt, intracardiac shunt, inadequate image quality,

and the presence of significant arrhythmias such as atrial fibrillation. Pediatric volunteers who met the inclusion criteria of the absence of known medical disease and normal electrocardiography were recruited through institutional website as control subjects. The decision to perform CMR for patients was based on clinical indications, including the presence of patient's symptoms and the need for cardiac and great arteries anatomic and functional assessment, in accordance with international guidelines.[18,19] For adult patients, 11 patients had Blalock-Taussig shunt before the intracardiac repair. For pediatric patients, no palliation was performed. The study protocols had been approved by SingHealth Centralised Institutional Review Board and the Institutional Review Board of Shanghai Children's Medical Center Affiliated to Shanghai Jiao Tong University School of Medicine. Written informed consent was obtained from all subjects or, where applicable, their parents or legal guardians.

In this study, only rTOF patients with 4D flow CMR were included, and then control groups without age and sex differences were selected accordingly. Hence, 103 rTOF patients (40 pediatric; 63 adult) and 62 healthy control subjects (15 pediatric; 47 adult) were included in the final analysis. In addition, RV systolic pressure was recorded from patients' echocardiographic report.

CMR PROTOCOL. CMR imaging protocols were standardized across sites. CMR scanners included: 3.0-T Ingenia (Philips Healthcare), 1.5-T Magneton Aera (Siemens Healthineers), and 3.0-T Discovery (GE Healthcare). Sedation was only given to pediatric patients under 6 years of age in accordance with departmental clinical protocol, but not to pediatric healthy subjects. 2D balanced steady-state free precession (bSSFP), short-axis cine images covering the LV and RV were acquired, along with 2-, 3-, and 4-chamber long-axis cine images. Cine images were acquired at 30 frames per cardiac cycle. Standard through-plane 2D PC PA flow measurement was acquired just above the pulmonary valve in a plane perpendicular to the long-axis of the pulmonary trunk, and aortic (AO) flow measurement was acquired in a single transverse plane that transected the proximal ascending aorta. Cine images and 2D PC flow sequences were acquired with breath-hold if possible. In patients with inconsistent breath-holding ability or inability to breath-hold, free-breathing sequences were performed instead. Free-breathing whole-heart 4D flow CMR was performed with respiratory-gating according to recommendations.[20,21] The typical temporal resolution was 30 to 41 ms. The VENC was 150 to 220 cm/s for the adult population and 160 to 200 cm/s for the pediatric population. Full standard cine, 2D PC, and 4D flow acquisition parameters for all scanners are provided in Supplemental Table 1.

CMR DATA ANALYSIS. CMR image analyses were performed at a core laboratory using MASS research software (Version 2022-EXP, Leiden University Medical Center).

Biventricular volume analysis. Artificial intelligence-assisted semiautomatic segmentation was performed for both LV and RV endocardial and epicardial borders in the short-axis stacks with visual checking and manual adjustment if needed.[22,23] Biventricular volume curves were generated for the entire cardiac cycle, and the maximal and minimal values of the volume curve were extracted as end-diastolic volume (EDV) and end-systolic volume (ESV), respectively. Papillary muscles and ventricular trabeculations were included in the volume calculation. The RV remodeling index was determined as the ratio of RVEDV to LVEDV.[24] Tricuspid regurgitation was visually graded as none, mild, moderate, or severe by experts (R.-S.T., Y.Z.) in RV outflow tract view[25] and compared with a recent echocardiogram, if available.

Tricuspid annular velocities and displacement. In-house software was used to semiautomatically track medial and lateral tricuspid valve insertions in the 4-chamber view. Peak systolic tricuspid velocity (S′) and tricuspid annular plane systolic excursion (TAPSE) were extracted from the velocity curve and displacement curve, respectively.[26,27]

2D and 4D flow analyses. By semiautomatically tracing the PA contours from 2D PC flow images, PR volume, PR fraction (PRF), PA maximal area, PA minimal area, and relative area change (RAC) were extracted from the generated MPA flow curve. RVRP was identified by the presence of end-diastolic forward flow during atrial contraction from the MPA curve. We denoted RVRP(+) as rTOF with RVRP and RVRP(−) as rTOF without RVRP. Similarly, AO forward flow and backward flow were calculated from the AO flow curve.

Error corrections and 4D flow quality checks were performed as previously reported.[23] The analysis techniques and definitions for biventricular 4D flow components (direct flow, retained inflow, delayed ejection flow, residual volume) and KE parameters normalized to EDV (global, peak systole, average systole, average diastole, peak E-wave, and peak A-wave KEi_{EDV}) have been described in our previous publications,[9,23,28,29] and the details are provided in the Supplemental Methods. KE discordance was defined as the ratio of RV average systolic KEi_{EDV} to

FIGURE 1 **Illustration of Parameters From 2D Phase-Contrast and 4D Flow CMR**

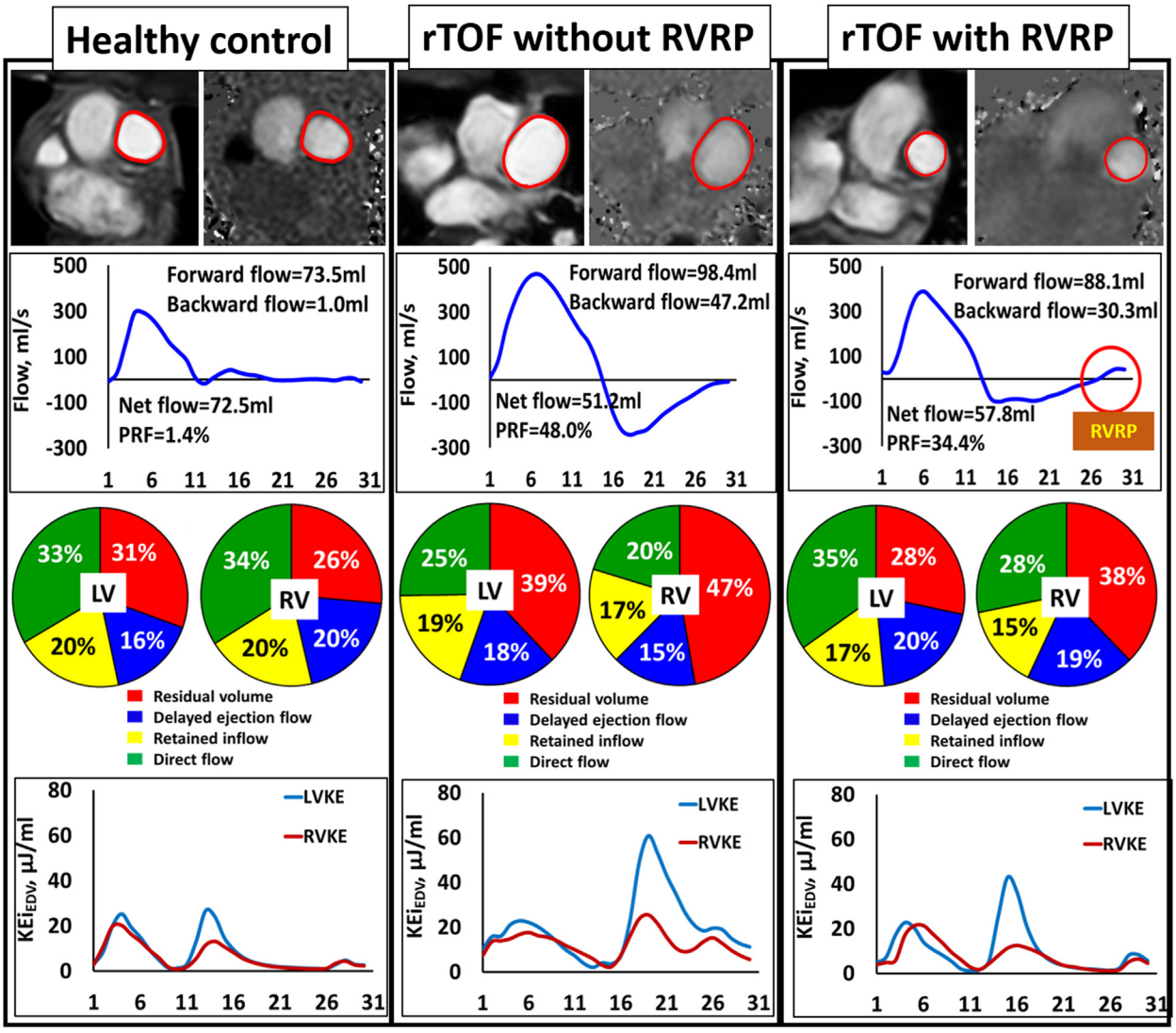

Segmentation of 2D phase-contrast main pulmonary artery borders was performed throughout the cardiac cycle (first row), and can generate the resultant pulmonary flow curve in MASS software (second row). Using 4D flow analysis, the 4 flow components for left ventricle (LV) and right ventricle (RV) can be calculated and displayed using pie plot (third row), and also the biventricular kinetic energy (KE) curves. We presented these in 1 healthy control (left panel), repaired tetralogy of Fallot (rTOF) without right ventricular restrictive physiology (RVRP) (middle panel) and rTOF with RVRP (right panel). KEi_{EDV} = kinetic energy normalized to end-diastolic volume; PRF = pulmonary regurgitant fraction.

LV average systolic KEi_{EDV}. Examples of 2D PC PA segmentation, resultant PA flow curve, biventricular flow components (pie plots), and KE curves in 1 healthy subject (left panel), 1 RVRP(−) (middle panel), and 1 RVRP(+) (right panel) are given in **Figure 1**.

CARDIOPULMONARY EXERCISE TEST. All adult subjects underwent cardiopulmonary exercise testing (CPET) at a central laboratory within 1 week after CMR using published protocols.[9,29] The details on calculations of peak oxygen uptake (PVO_2), metabolic equivalents (METs), % predicted PVO_2, and minute ventilation (VE)/carbon dioxide output (VCO_2) are provided in the Supplemental Methods.

STATISTICAL ANALYSIS. Data were analyzed using SPSS (version 25.0). Continuous variables were expressed as mean ± SD if normally distributed or median (25th percentile, 75th percentile) if non-normally distributed, and category data were

represented as n (%). Comparison of means between 2 independent groups was assessed using the 2-sample Student's *t*-test for normally distributed data and Mann-Whitney *U* test for non-normally distributed data. Kruskal-Wallis nonparametric 1-way analysis of variance analysis was used for more than 2 groups with post hoc pair-wise comparisons in the event of a significant Kruskal-Wallis test. Either the chi-square test or Fisher exact test, as appropriate, was used for analysis of categorical variables. Binary logistic regression analysis was used to identify independent predictors of RVRP. Statistical significance was set at $P < 0.05$.

RESULTS

DEMOGRAPHICS AND BASELINE CHARACTERISTICS. Table 1 presents baseline characteristics of our study population. The mean age of rTOF patients was 24 years, with 50 of 103 (48.5%) female patients, and healthy control subjects had mean age of 24 years of age with 31 of 62 (50.0%) female patients. The median age of patients having performed their primary TOF repair was 2.0 years old, and 85 of 103 (82.5%) patients had transannular patch repair (35 pediatric and 50 adult subjects). For rTOF patients, 12 of 103 (11.6%) had moderate to severe tricuspid regurgitation (3 pediatric and 9 adult subjects) and 2 of 103 (1.9%) had reintervention (0 pediatric and 2 adult subjects, all of whom had pulmonary valve replacement). In total, 70 of 103 (68%) patients had RVRP (25 pediatric and 45 adult subjects), and the median ages of RVRP(−) and RVRP(+) were 21 and 28 years, respectively. No significant differences were observed in heart rate and surgical history between RVRP(−) and RVRP(+) (Table 1) and between pediatric and adult rTOF (Supplemental Table 2).

DIFFERENCES IN CONVENTIONAL CMR AND EXERCISE PARAMETERS. Compared with control subjects, rTOF patients had significantly dilated RV with increased RV mass index and RV mass/LV mass; impaired LV/RV function in terms of LV ejection fraction (LVEF), right ventricular ejection fraction (RVEF), S', and TAPSE; adverse RV remodeling (RVEDV/LVEDV); and smaller LV stroke volume index (Table 1). PA minimal area was larger and RAC was smaller in rTOF patients. rTOF patients had significantly reduced PVO_2, METs, % predicted PVO_2, and increased VE/VCO_2 slope compared with control subjects.

RVRP(+) had significantly larger RVSV index and RVEDV/LVEDV, smaller LVEDV index and LVESV index, and better LVEF, RVEF, and TAPSE in comparison to RVRP(−) (Table 1). There were no differences in PA dimensions (PA maximal, minimal areas and RAC) between RVRP(−) and RVRP(+). The pulmonary regurgitation fraction increased in RVRP(+) compared with RVRP(−), although there were no significant differences in PVO_2, METs, and % predicted PVO_2 between RVRP(+) and RVRP(−) patients, with significantly higher VE/VCO_2 slope in RVRP(+).

In contrast to pediatric rTOF, adult rTOF exhibited significantly elevated indexed values of RVEDV, RVESV, RVSV and LV mass, RVEDV/LVEDV, and LVEF, along with significantly lower LVEDV index, LVESV index, and RV mass/LV mass (Supplemental Table 2). Pediatric rTOF had smaller PA maximal and minimal areas and higher PA relative area change. The pulmonary regurgitation fraction was comparable between pediatric and adult rTOF patients.

DIFFERENCES IN 4D FLOW PARAMETERS. Table 2 presents the biventricular flow components and KE parameters between control and rTOF patients and between RVRP(−) and RVRP(+). In the RV, rTOF patients had significantly reduced direct flow and increased delayed ejection flow and residual volume compared with control subjects. rTOF patients had significantly elevated RV global, peak systolic, systolic, diastolic, and peak E-wave KEi_{EDV}; E-wave/A-wave; and KE discordance. However, in the LV, rTOF patients had significantly lower direct flow and had higher retained inflow and diastolic and peak E-wave KEi_{EDV}.

Compared with RVRP(−), RVRP(+) exhibited increased RV direct flow, RV peak E-wave KEi_{EDV}, RV E-wave/A-wave, and reduced RV residual volume, LV global and diastolic KEi_{EDV} (Table 2). Compared with pediatric patients, adult rTOF patients displayed elevated levels of peak systolic, systolic, peak E-wave, and peak A-wave KEi_{EDV} in the LV, along with increased retained inflow, diastolic, and peak E-wave KEi_{EDV} in the RV and lower KE discordance (Supplemental Table 2).

4D FLOW PARAMETERS ON RV RESTRICTIVE PHYSIOLOGY. In pediatric population (Figure 2, left panel), pediatric control and pediatric RVRP(+) had comparable RV direct flow (respectively RV residual volume), with significant decrease (respectively increase) in pediatric RVRP(−). Both pediatric RVRP(−) and pediatric RVRP(+) had significant increase in RV peak E-wave KEi_{EDV} and KE discordance, with no differences between the 2 groups. In the adult population (Figure 2, right panel), both RVRP(−) and RVRP(+) had significantly reduced RV direct flow and increased RV residual volume compared with the control group; there was a significant increase trend in RV peak

TABLE 1 Comparison of Demographics, CMR, and CPET Parameters

	Control (n = 62)	rTOF (n = 103)	*P* Value	rTOF Without RVRP (n = 33)	rTOF With RVRP (n = 70)	*P* Value
Demographics						
Age at CMR scan, y	24 ± 9	24 ± 17	0.899	21 (9, 27)	28 (8, 38)	0.145
Age of primary repair, y	–	2.0 (0.8, 4.0)	–	1.3 (0.6, 3.0)	2.0 (0.9, 4.3)	0.325
Male/female	31/31	53/50	0.874	17/16	36/34	1.000
Height, cm	162 ± 15	148 ± 28	**<0.001**	150 ± 30	147 ± 27	0.612
Weight, kg	58 ± 18	49 ± 25	**0.006**	51 ± 26	48 ± 24	0.516
Body surface area, m^2	1.61 ± 0.31	1.39 ± 0.47	**<0.001**	1.43 ± 0.51	1.37 ± 0.46	0.536
Heart rate, beats/min	75 ± 13	77 ± 11	0.497	79 ± 11	76 ± 11	0.150
Types of repair[a]						0.611
Transannular patch	–	85 (82.5)	–	26 (78.8)	59 (84.3)	
Valve-sparing	–	unknown	–	Unknown	Unknown	
Conduit	–	5 (4.9)	–	2 (6.1)	3 (4.3)	
Tricuspid regurgitation						0.271
No	62 (100)	60 (58.3)	–	22 (66.7)	38 (54.3)	
Mild	–	31 (30.1)	–	7 (21.2)	24 (34.3)	
Moderate to severe	–	12 (11.6)	–	4 (12.2)	8 (11.4)	
Numbers with reintervention	–	2 (1.9)	–	2 (1.9)	0 (0.0)	–
Pulmonary valve replacement	–	2 (1.9)	–	2 (1.9)	0 (0.0)	–
RVRP	–	70 (68.0)	–			
Right ventricular systolic pressure, mm Hg	–	50 (26, 39)	–	33 (27, 42)	30 (26, 37)	0.215
LV function						
LV mass index, g/m^2	45 ± 9	44 ± 14	0.563	45 ± 15	43 ± 13	0.508
LV EDV index, mL/m^2	76 ± 13	72 ± 13	0.051	77 ± 14	69 ± 12	**0.002**
LV ESV index, mL/m^2	30 ± 9	30 ± 10	0.677	35 ± 11	28 ± 8	**<0.001**
LV stroke volume index, mL/m^2	46 ± 8	41 ± 7	**<0.001**	42 ± 7	41 ± 7	0.426
LVEF, %	61 ± 8	58 ± 9	**0.024**	55 ± 9	60 ± 8	**0.011**
RV function						
RV EDV index, mL/m^2	82 ± 14	127 ± 32	**<0.001**	122 ± 38	130 ± 29	0.275
RV ESV index, mL/m^2	38 ± 10	67 ± 22	**<0.001**	68 ± 26	66 ± 19	0.651
RV stroke volume index, mL/m^2	44 ± 7	61 ± 16	**<0.001**	54 ± 17	64 ± 14	**0.004**
RVEF, %	54 ± 7	48 ± 8	**<0.001**	45 ± 9	50 ± 7	**0.011**
RVEDV/LVEDV	1.08 ± 0.09	1.83 ± 0.57	**<0.001**	1.62 ± 0.49	1.94 ± 0.57	**0.007**
RV mass index, g/m^2	16.5 ± 2.8	28.6 ± 7.2	**<0.001**	28.5 ± 6.9	28.7 ± 7.5	0.871
RV mass/LV mass	0.38 ± 0.09	0.68 ± 0.18	**<0.001**	0.67 ± 0.21	0.69 ± 0.17	0.586
S', cm/s	10.4 ± 2.2	6.9 ± 1.9	**<0.001**	6.7 ± 1.9	7.1 ± 1.9	0.348
TAPSE, mm	19.7 ± 3.4	12.9 ± 3.8	**<0.001**	11.8 ± 3.6	13.4 ± 3.8	**0.046**
2D phase-contrast flow						
PA maximal area, cm^2	6.9 ± 1.8	7.3 ± 2.6	0.226	7.0 ± 2.8	7.5 ± 2.6	0.404
PA minimal area, cm^2	4.2 ± 1.6	4.9 ± 2.0	**0.019**	4.6 ± 1.9	5.0 ± 2.1	0.274
Relative area change, %	71 ± 24	58 ± 36	**0.017**	60 ± 32	57 ± 38	0.794
PA forward flow, mL	68.8 (63.1, 82.0)	88.3 (57.9, 112.5)	**0.007**	75.0 (51.6, 98.9)	93.8 (61.0, 114.4)	0.136
Pulmonary net flow, mL	68.1 (61.8, 80.3)	49.0 (29.5, 62.5)	**<0.001**	48.9 (25.8, 64.7)	49.1 (32.1, 60.1)	0.611
Pulmonary regurgitant volume, mL	0.63 (0.20, 1.49)	35.1 (18.8, 57.9)	**<0.001**	25.3 (12.9, 42.7)	40.6 (26.4, 61.1)	**0.004**
Pulmonary regurgitant fraction, %	1.0 (0.3, 2.0)	44.7 (34.5, 53.6)	**<0.001**	37.8 (25.4, 49.3)	47.0 (38.6, 55.7)	**0.003**
Aortic forward flow, mL	67.8 (60.1, 80.6)	53.7 (35.9, 67.7)	**<0.001**	54.0 (33.2, 70.4)	53.4 (36.8, 67.7)	0.805
Aortic net flow, mL	67.2 (59.9, 79.8)	52.4 (34.8, 64.7)	**<0.001**	49.2 (31.0, 69.3)	52.4 (35.5, 63.4)	0.927
Aortic regurgitant fraction, %	0.6 (0.2, 1.1)	1.9 (1.1, 4.2)	**<0.001**	2.5 (1.2, 5.1)	1.7 (1.0, 3.7)	0.190
CPET[b]						
PVO_2, mL/kg/min	24.5 (20.8, 29.1)	18.1 (14.9, 21.8)	**<0.001**	18.1 (13.7, 23.5)	18.4 (15.6, 21.8)	0.553
METs	7.0 (5.9, 8.3)	5.2 (4.3, 6.2)	**<0.001**	5.2 (3.9, 6.7)	5.1 (4.5, 6.2)	0.553
% predicted PVO_2, %	86 (70, 111)	68 (56, 82)	**<0.001**	65 (53, 71)	70 (60, 83)	0.126
VE/VCO_2 slope	25 (24, 27)	27 (25, 30)	**0.003**	25 (24, 29)	28 (25, 31)	**0.026**

Values are mean ± SD, n (%), or median (25th percentile, 75th percentile). **Bold** indicates statistical significance. [a]Type of repair data missing in 10 repaired tetralogy of Fallot (rTOF) patients. [b]Cardiopulmonary exercise testing (CPET) is only available in 47 healthy adults and 63 adult rTOF.

CMR = cardiovascular magnetic resonance; EDV = end-diastolic volume; ESV = end-systolic volume; KE = kinetic energy; KE discordance = right ventricular/left ventricular systolic KEi_{EDV}; KEi_{EDV} = kinetic energy normalized to end-diastolic volume; LV = left ventricle; LVEF = left ventricular ejection fraction; METs = metabolic equivalents; PA = pulmonary artery; PVO_2 = peak oxygen uptake; RV = right ventricle; RVEF = right ventricular ejection fraction; RVRP = right ventricular restrictive physiology; S' = peak systolic tricuspid velocity by CMR feature tracking; TAPSE = tricuspid annular plane systolic excursion by CMR feature tracking; VCO_2 = carbon dioxide output; VE = minute ventilation.

JACC: ASIA, VOL. 4, NO. 12, 2024
DECEMBER 2024:912–924

TABLE 2 Comparison of 4D Flow Parameters Between Control and rTOF, and rTOF Without and With RVRP

	Control (n = 62)	rTOF (n = 103)	*P* Value	rTOF Without RVRP (n = 33)	rTOF With RVRP (n = 70)	*P* Value
LV flow components						
Direct flow, %	34 (29, 40)	30 (26, 36)	**0.007**	28 (24, 37)	31 (28, 36)	0.252
Retained inflow, %	14 (12, 17)	19 (14, 22)	**<0.001**	19 (14, 22)	18 (14, 21)	0.858
Delayed ejection flow, %	18 (15, 22)	18 (15, 21)	0.722	18 (15, 22)	17 (14, 20)	0.216
Residual volume, %	33 (29, 37)	31 (28, 36)	0.419	31 (27, 37)	31 (28, 36)	0.852
LV kinetic energy parameters						
Global KEi_{EDV}, μJ/mL	10.3 (7.7, 12.0)	11.0 (8.7, 13.5)	0.056	11.8 (10.8, 14.8)	10.4 (8.4, 12.3)	**0.007**
Peak systolic KEi_{EDV}, μJ/mL	18.4 (15.6, 22.8)	16.9 (12.7, 22.8)	0.125	17.2 (14.0, 27.8)	16.9 (12.4, 21.4)	0.248
Systolic KEi_{EDV}, μJ/mL	10.0 (8.5, 13.0)	9.2 (7.4, 12.6)	0.235	9.7 (8.6, 14.7)	9.1 (7.1, 11.3)	0.083
Diastolic KEi_{EDV}, μJ/mL	9.5 (7.4, 12.4)	11.6 (9.2, 14.9)	**0.001**	12.7 (10.9, 16.3)	11.1 (8.5, 13.6)	**0.019**
Peak E-wave KEi_{EDV}, μJ/mL	30.0 (24.8, 35.9)	34.4 (26.1, 44.8)	**0.016**	36.4 (27.8, 46.3)	32.7 (25.4, 44.9)	0.375
Peak A-wave KEi_{EDV}, μJ/mL	9.6 (6.8, 11.6)	8.2 (5.7, 13.2)	0.371	9.4 (6.3, 15.9)	7.9 (5.4, 10.6)	0.089
KEi_{EDV} E-wave/A-wave	3.37 (2.48, 4.66)	3.74 (2.66, 6.01)	0.088	3.11 (2.41, 5.95)	4.23 (2.77, 6.01)	0.161
RV flow components						
Direct flow, %	35 (29, 40)	26 (19, 30)	**<0.001**	20 (15, 28)	27 (22, 31)	**0.002**
Retained inflow, %	16 (13, 18)	16 (13, 19)	0.599	16 (14, 19)	16 (13, 19)	0.429
Delayed ejection flow, %	17 (14, 20)	19 (15, 23)	**0.017**	19 (15, 24)	20 (16, 23)	0.822
Residual volume, %	30 (27, 37)	38 (34, 44)	**<0.001**	42 (34, 52)	37 (33, 42)	**0.039**
RV kinetic energy parameters						
Global KEi_{EDV}, μJ/mL	9.2 (7.9, 11.4)	14.2 (11.4, 18.0)	**<0.001**	13.2 (11.6, 16.9)	14.5 (11.2, 18.2)	0.673
Peak systolic KEi_{EDV}, μJ/mL	24.5 (19.8, 28.3)	29.2 (21.4, 40.8)	**0.001**	25.2 (20.3, 41.3)	30.0 (22.6, 41.2)	0.212
Systolic KEi_{EDV}, μJ/mL	13.3 (11.6, 15.8)	17.1 (13.7, 22.4)	**<0.001**	17.9 (14.2, 21.7)	16.5 (13.5, 23.1)	0.867
Diastolic KEi_{EDV}, μJ/mL	6.8 (5.5, 8.7)	11.8 (8.6, 15.1)	**<0.001**	11.2 (8.8, 13.9)	12.2 (8.4, 16.8)	0.421
Peak E-wave KEi_{EDV}, μJ/mL	14.0 (11.6, 18.5)	25.7 (16.2, 35.4)	**<0.001**	20.7 (14.3, 30.3)	28.4 (17.1, 36.8)	**0.015**
Peak A-wave KEi_{EDV}, μJ/mL	7.2 (5.1, 10.0)	7.6 (5.4, 12.3)	0.159	8.7 (5.0, 16.9)	7.2 (5.4, 11.2)	0.283
KEi_{EDV} E-wave/A-wave	1.86 (1.22, 2.99)	2.87 (1.67, 4.30)	**0.001**	1.47 (1.12, 3.21)	3.33 (2.27, 4.34)	**0.009**
KE discordance	1.27 (1.13, 1.47)	1.79 (1.22, 2.34)	**<0.001**	1.52 (1.08, 2.28)	1.86 (1.41, 2.37)	0.086

Values are median (25th percentile, 75th percentile). **Bold** indicates statistical significance.
Abbreviations as in Table 1.

E-wave KEi_{EDV} from control to RVRP(−) to RVRP(+), with only RVRP(+) having significantly higher KE discordance than control.

On multivariable binary logistic analysis, only RVEDV/LVEDV (OR: 7.664; 95% CI: 2.419-24.282; $P = 0.001$) and RV direct flow (OR: 1.158; 95% CI: 1.074-1.249; $P < 0.001$) were independently associated with rTOF with RV restrictive physiology after adjusting age and CMR cine (LVEF, RVEF, RVEDV/LVEDV, CMR feature tracking derived peak systolic tricuspid velocity, and TAPSE) and 2D PC parameters (pulmonary regurgitant fraction, pulmonary artery relative area change) (Table 3).

DISCUSSION

This is the first study to explore the relationship between flow components and kinetic energy parameters derived from 4D flow CMR and RV restrictive physiology in an rTOF cohort including both pediatric and adult subjects. Although RV direct flow decreased in rTOF patients compared with healthy control subjects, it was higher in rTOF with RVRP compared with those without RVRP, and moreover, it was independently associated with RV restrictive physiology in rTOF (Central Illustration).

4D FLOW COMPONENTS AND KE IN rTOF. The analysis of ventricular flow components and KE parameters revealed distinctive patterns in rTOF patients compared with healthy control subjects. Consistent with prior publication,[10] our findings demonstrated an elevation in RV KE parameters, encompassing global, peak systolic, systolic, diastolic, peak E-wave, and KE discordance. RV diastolic KE is increased because of the augmented pulmonary regurgitation component,[11] while the resultant increase in ventricular preload contributes to increased RV systolic KE. In terms of RV flow components, there was reduced direct flow and increased delayed ejection flow and residual volume, which was in agreement with our previous study.[9] Our findings also demonstrated altered LV KE parameters in rTOF patients, with increased LV diastolic and peak E-wave KE. In line

FIGURE 2 **Bar Plot Comparisons of RV 4D Flow Parameters**

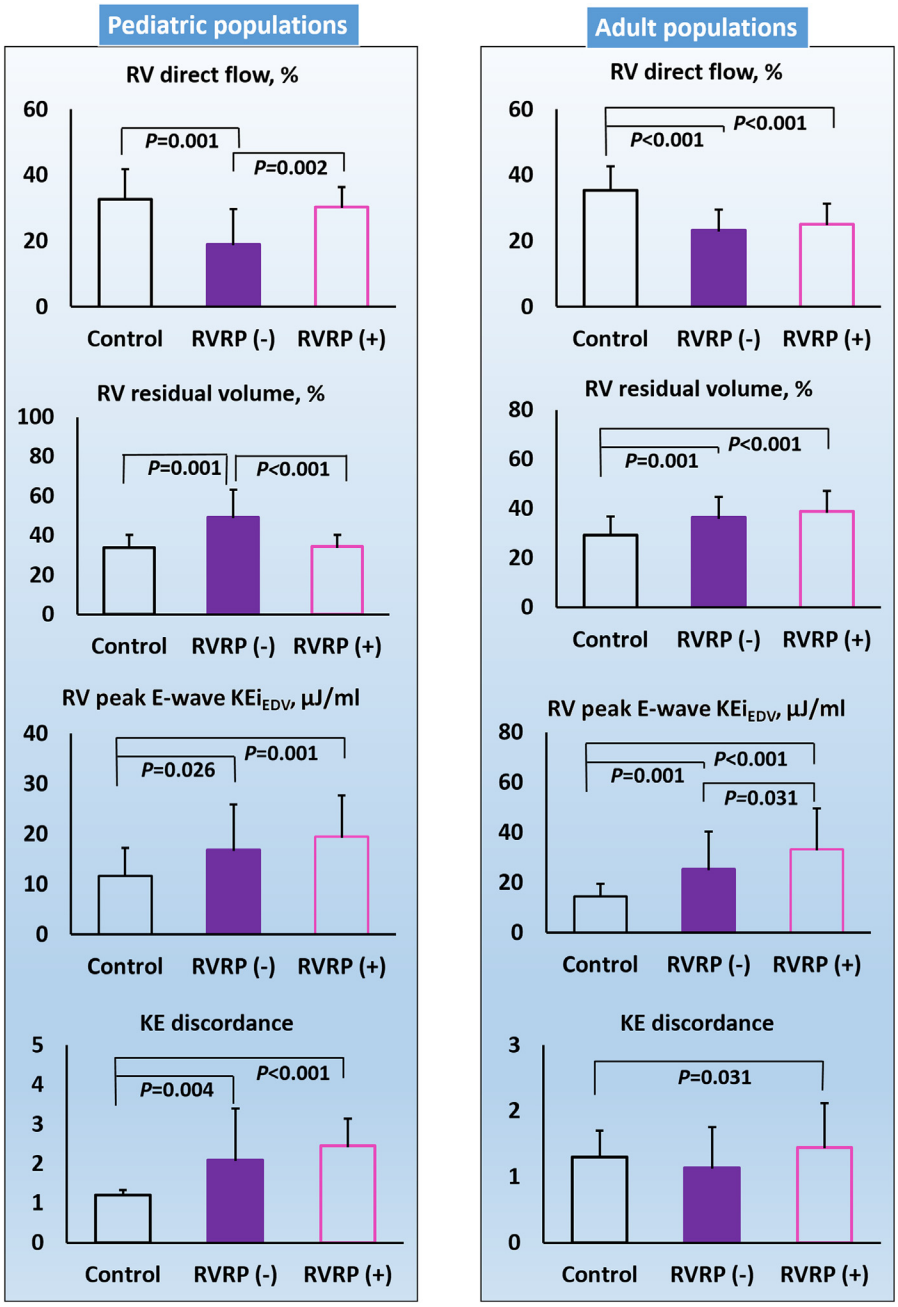

Kruskal-Wallis nonparametric 1-way analysis of variance analysis was used to compare the 3 subgroups, with post hoc pairwise comparisons. In the event of a significant Kruskal-Wallis test without any correction, only raw *P* values were reported. Comparisons of RV direct flow (first row), RV residual volume (second row), RV peak E-wave KEi_{EDV} (third row) and KE discordance (last row) among control, rTOF without and with RVRP for pediatric and adult subjects were given on the left panel and right panel, respectively. RVRP (−) = rTOF without RVRP; RVRP (+) = rTOF with RVRP; other abbreviations as in Figure 1.

TABLE 3 Univariate and Multivariable Binary Logistic Regression Analysis for Determinants of RV Restrictive Physiology in rTOF

	Univariate Analysis		Multivariable Analysis	
	OR (95% CI)	*P* Value	OR (95% CI)	*P* Value
Age, y	1.019 (0.992–1.046)	0.168	–	
LVEF, %	1.074 (1.014–1.138)	0.015	–	
RVEF, %	1.087 (1.023–1.156)	0.007	–	
RVEDV/LVEDV	3.507 (1.383–8.889)	**0.008**	**7.664 (2.419–24.282)**	**0.001**
Pulmonary regurgitant fraction, %	1.044 (1.013–1.076)	0.005	–	
PA relative area change, %	0.998 (0.987–1.010)	0.791	–	
S', cm/s	1.116 (0.889–1.400)	0.345	–	
TAPSE, mm	1.127 (1.000–1.270)	0.049	–	
RV direct flow, %	1.109 (1.043–1.180)	**0.001**	**1.158 (1.074–1.249)**	**<0.001**
RV retained inflow, %	0.963 (0.876–1.059)	0.435	–	
RV delayed ejection flow, %	1.025 (0.953 1.101)	0.510	–	
RV residual volume, %	0.940 (0.899–0.984)	0.008	–	
RV global KEi_{EDV}, μJ/mL	1.032 (0.958–1.113)	0.407	–	
RV peak systolic KEi_{EDV}, μJ/mL	1.015 (0.984–1.046)	0.345	–	
RV systolic KEi_{EDV}, μJ/mL	1.007 (0.958–1.058)	0.788	–	
RV diastolic KEi_{EDV}, μJ/mL	1.052 (0.973–1.137)	0.203	–	
RV peak E-wave KEi_{EDV}, μJ/mL	1.036 (1.001–1.073)	0.042	–	
RV peak A-wave KEi_{EDV}, μJ/mL	0.954 (0.887–1.026)	0.200	–	
RV KEi_{EDV} E-wave/A-wave	1.232 (0.930–1.631)	0.145	–	
KE discordance	1.255 (0.760–2.071)	0.375	–	
Cox and Snell R-squared, multivariable				0.242
Nagelkerke R-squared, multivariable				0.336

Bold indicates statistical significance.
Abbreviations as in Table 1.

with a prior study,[30] we also observed reduced LV systolic peak KE in rTOF, but not reaching statistical significance after normalizing to LVEDV. The cause of altered LV KE parameters and flow components observed in our study is unclear, perhaps related to ventricular interdependence described within this patient population[31] and septal dyssynchrony with septal movement toward the RV in systole.[32]

RV RESTRICTIVE PHYSIOLOGY IN rTOF. There have been several studies investigating the RV restrictive physiology either in pediatric or adult rTOF. Apitz et al[33] found that diastolic RV stiffness, characterized by end-diastolic pressure-volume relationship, increased in RVRP(+) among 25 children and adolescents. In 50 patients with exercise test, Lee et al[34] showed that the presence of end-diastolic forward flow is associated with better % predicted PVO_2 only in patients with RVEDV index <170 mL/m^2. Similarly, Cavalho et al[35] showed that RVRP could reduce PR caused by RV restriction, leading to better physical activity in 12 pediatric patients. In 41 patients aged 15-35 years (31 patients with treadmill exercise), Gatzoulis et al.[4] showed that RVRP(+) achieved a significantly higher % predicted PVO_2 compared with RVRP(−) (100.5% vs 82.6%; $P < 0.001$). In our study, we also observed an increase trend in % predicted PVO_2 (median values: 70% vs 65%; $P = 0.126$), and our values were smaller compared with those in Gatzoulis et al,[4] possibly because of the different age range between 2 studies. While another study showed that RVRP had no contributing effect on exercise capacity in terms of maximal heart rate attained, maximum predicted heart rate, and METs in 80 pediatric rTOF patients (mean age 7.9 years).[3] As our pediatric subjects did not perform exercise testing, no comparison with existing studies can be made here. Our results showed no significant differences in majority of CPET parameters (PVO_2, METs, and % predicted PVO_2). Unexpectedly, VE/VCO_2 slope was higher in RVRP(+). This suggests reduced ventilatory efficiency in RVRP(+), and is contradictory to the postulated benefits of RVRP. Future studies are warranted to provide more evidence on the effect of RVRP on exercise capacity in rTOF either in pediatrics or adults, or both.

INSIGHTS INTO RVRP USING 4D FLOW CMR IN rTOF. For the first time, biventricular flow components and KE parameters using 4D flow CMR were compared in rTOF with and without RVRP. Despite higher pulmonary regurgitation volume and fraction in RVRP(+), they paradoxically had lower RV residual volume

CENTRAL ILLUSTRATION **Right Ventricular Direct Flow Associated With Right Ventricular Restrictive Physiology in Repaired Tetralogy of Fallot**

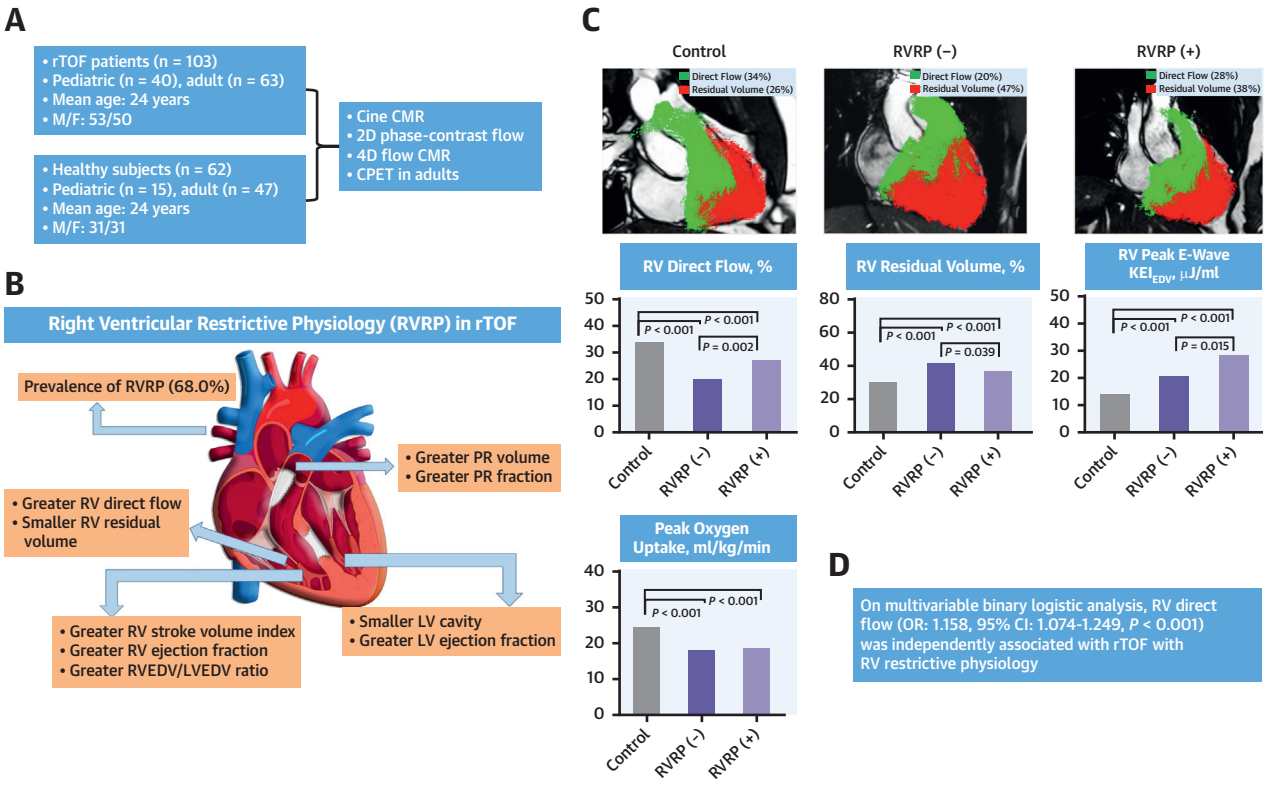

Zhao X, et al. JACC Asia. 2024;4(12):912–924.

(A) A total of 103 patients with rTOF and 62 healthy control subjects were included in the study. (B) Patients with RVRP have greater PR volume and PR fraction; smaller LV cavity; greater LV ejection fraction; greater RV stroke volume index, RV ejection fraction, RVEDV/LVEDV ratio, and RV direct flow; and smaller RV residual volume. (C) Patients with RVRP have increased RV direct flow, deceased residual volume, and increased peak E-wave KEi$_{EDV}$ compared with patients without RVRP. (D) On multivariable binary logistic analysis, RV direct flow was independently associated with RVRP (OR: 1.158). CMR = cardiovascular magnetic resonance; CPET = cardiopulmonary exercise test; LV = left ventricle; LVEDV = left ventricular end-diastolic volume; KEi$_{EDV}$ = kinetic energy normalized to end-diastolic volume; PR = pulmonary regurgitation; rTOF = repaired Tetralogy of Fallot; RV = right ventricle; RVEDV = right ventricular end-diastolic volume; RVRP(–) = rTOF without RVRP; RVRP(+) = rTOF with RVRP.

compared with RVRP(–). Noninvasive measurements of ventricular KE utilizing 4D flow acquisitions provided a nondirectional measure of the amount of work invested in overcoming the inertia of intracardiac blood during the cardiac cycle.[36,37] RV diastolic dysfunction might be an earlier,[38] more prominent feature of maladaptation than systolic dysfunction, and abnormal diastolic flow patterns were consistently present while systolic flow was preserved in most rTOF with PR.[39] In terms of KE parameters, we found that RV peak E-wave KEi$_{EDV}$ increased more in RVRP(+), whereas a previous study showed more pronounced increase in diastolic peak KE/stroke volume in RVRP(–).[30] Moreover, their RV diastolic peak might have a different relationship with our peak E-wave KE. Except for peak E-wave KE, there were no discernible differences in RV KE parameters between RVRP subgroups. This suggests that the RV in RVRP(+) required a similar workload to that of RVRP(–) individuals, even in the presence of considerably more PR. The underlying cause of this phenomenon is uncertain; however, it is conceivable that the anticipated RV remodeling and hypertrophy in RVRP(+) patients might mitigate ventricular wall stress in accordance to the Law of Laplace.[40]

We also performed ventricular flow components and kinetic energy parameters comparison analysis among control volunteers, among patients with and without RVRP, and in pediatric and adult cohorts. Both adult and pediatric RVRP(–) have lower RV

direct flow and higher RV residual volume and RV peak E-wave compared with corresponding control volunteers. Between patient groups, we found that pediatric RVRP(+) had higher RV direct flow and lower RV residual volume than pediatric RVRP(−) (Figure 2). In contrast, RV direct flow and RV residual volume were similar between adult RVRP(+) and adult RVRP(−). In addition, RV peak E-wave were higher in adult RVRP(+) compared with adult RVRP(−). These preliminary results might provide insights into the understanding of RV adaption and remodeling as patients transition from pediatric to adult age groups.

CLINICAL PERSPECTIVES AND IMPLICATIONS. Conventional CMR parameters, including RVEDV and RVESV index, ejection fraction, cardiac index, and ventricular mass index, have been established as correlates of disease severity and prognostic indicators in rTOF.[41,42] These parameters focus on ventricular anatomy and ejection fraction but lack hemodynamic data, often necessitating an invasive cardiac catheterization to quantify ventricular filling pressure and pulmonary arterial resistance. With the accumulation of more 4D flow research data, it is highly likely that we will include 4D flow-derived hemodynamic data in the decision matrix for managing rTOF patients in the future. Therefore, it is important to add our study to the growing body of evidence in this area. The use of 4D flow to assess ventricular flow components and kinetic energy parameters in the management of rTOF patients is novel, and our study adds to the growing evidence of incorporating 4D flow data in this patient population.[9,10,18,30,41] To increase adoption in clinical practice, we will need to establish optimal severity grading values for ventricular flow components and KE parameters for 4D flow CMR in this population. In rTOF patients who require regular surveillance imaging, a significant advantage of the use of 4D flow CMR is that comprehensive, accurate hemodynamic data can be obtained without radiation. The novel hemodynamic parameters reveal underlying mechanisms of cardiac diseases and show promise for future clinical application, although they currently remain within the realm of research. Fundamentally, we need large, multicenter, longitudinal studies to assess the clinical validity of these parameters in the management of rTOF patients.

STUDY LIMITATIONS. The collective evidence from our study and prior publication underscores the need for future research to determine the predictive power of KE measurements and ventricular flow components for clinical outcomes such as patient's morbidity, mortality, RV dysfunction, and the optimal timing of reintervention. The lack of such outcomes in our study is the main limitation and warrants further research. Inherent technical limitations associated with 4D flow CMR are extensively documented and discussed in the published reports.[7,20] Another limitation is the lack of exercise testing in pediatric subjects. We are in the process of setting up an exercise machine for our pediatric populations, and will investigate the relationships among 4D flow, RVRP, and exercise in future studies. The assessment of ventricular flow components and KE requires specialized software packages, which may not be routinely available in standard postprocessing software for clinical practice. Existing technical constraints encompass extended scan durations and protracted assessments, with a routine clinical TOF CMR protocol utilizing 45 minutes and an additional 10 to 20 minutes for 4D flow acquisition. Nonetheless, it is important to note that ongoing advancements are continually addressing these limitations, such as accelerated imaging protocols like compressed sensing,[43] and deep-learning image reconstruction,[44] holding the promise of overcoming these challenges in the future. At present, the cine spatial resolution of the ventricular cavity acquired in 4D flow CMR is limited, necessitating the use of bSSFP ventricular short-axis cine images for quantification of ventricular volume and function. Despite this limitation, studies have shown that ventricular volumes and pulmonary flow measured with 4D flow CMR are comparable to those obtained with 2D bSSFP cine[45] and 2D phase-contrast imaging.[46] With technological advancements leading to improved structural spatial resolution in 4D flow, it is possible that a complete CMR study could eventually be performed in a single 4D flow sequence, significantly reducing scan times. Last, we used the presence of end-diastolic forward flow during atrial contraction in the PA flow curve as the definition of RV restrictive physiology, although in a meta-analysis,[47] the authors suggested that EDFF may have multiple causes and might not be the precise equivalent of RVRP.

CONCLUSIONS

Our study provides a deeper understanding of the intricate relationships among 4D flow parameters, right ventricular hemodynamics, and restrictive physiology in individuals with rTOF. These findings offer valuable insights into the management and

prognostication of rTOF patients, and provide directions for future research on the impact of RVRP in rTOF using 4D flow CMR with clinical outcomes.

FUNDING SUPPORT AND AUTHOR DISCLOSURES

This work was supported by the National Medical Research Council of Singapore (NMRC/OFIRG/0018/2016, MOH-000358, MOH-000351), National Natural Science Foundation of China (No. 82171902), and Shanghai Committee of Science and Technology (No. 21Y11910700). The authors have reported that they have no relationships relevant to the contents of this paper to disclose.

ADDRESS FOR CORRESPONDENCE: Dr Yumin Zhong, Department of Radiology, Shanghai Children's Medical Center, Shanghai Jiao Tong University School of Medicine, 1678 Dongfang Road, 200127 Shanghai, China. E-mail: zyumin2002@163.com. OR Dr Liang Zhong, National Heart Research Institute Singapore, National Heart Centre Singapore, 5 Hospital Drive, 169609 Singapore. E-mail: zhong.liang@duke-nus.edu.sg.

PERSPECTIVES

COMPETENCY IN MEDICAL KNOWLEDGE: For the first time, biventricular flow components and KE derived from 4D flow CMR were compared between rTOF with and without RVRP including both pediatric and adult subjects. rTOF with RVRP had increased RV direct flow and reduced RV residual volume compared with those without RVRP, and exercise capacity was compared between 2 groups in adult subjects. On multivariable binary logistic regression analysis, we found that RV direct flow was an independent marker of rTOF with RVRP.

TRANSLATIONAL OUTLOOK: In the pediatric group, RV direct flow was comparable between rTOF with RVRP and control, whereas in adult group, RV direct flow was significantly decreased in rTOF with RVRP compared with control subjects. Therefore, future longitudinal study is warranted to investigate the ventricular flow hemodynamic changes from pediatric to adult rTOF patients to better understand young-old adaptive progression in this cohort.

REFERENCES

1. Apitz C, Webb GD, Redington AN. Tetralogy of Fallot. *Lancet Lond Engl*. 2009;374:1462–1471.

2. Cullen S, Shore D, Redington A. Characterization of right ventricular diastolic performance after complete repair of tetralogy of Fallot. Restrictive physiology predicts slow postoperative recovery. *Circulation*. 1995;91:1782–1789.

3. Rathore KS, Agrawal SK, Kapoor A. Restrictive physiology in tetralogy of Fallot: exercise and arrhythmogenesis. *Asian Cardiovasc Thorac Ann*. 2006;14:279–283.

4. Gatzoulis MA, Clark AL, Cullen S, Newman CG, Redington AN. Right ventricular diastolic function 15 to 35 years after repair of tetralogy of Fallot. Restrictive physiology predicts superior exercise performance. *Circulation*. 1995;91:1775–1781.

5. Ahmad N, Kantor PF, Grosse-Wortmann L, et al. Influence of RV restrictive physiology on LV diastolic function in children after tetralogy of Fallot repair. *J Am Soc Echocardiogr*. 2012;25:866–873.

6. Helbing WA, Niezen RA, Le Cessie S, van der Geest RJ, Ottenkamp J, de Roos A. Right ventricular diastolic function in children with pulmonary regurgitation after repair of tetralogy of Fallot: volumetric evaluation by magnetic resonance velocity mapping. *J Am Coll Cardiol*. 1996;28:1827–1835.

7. Bissell MM, Raimondi F, Ait Ali L, et al. 4D Flow cardiovascular magnetic resonance consensus statement: 2023 update. *J Cardiovasc Magn Reson*. 2023;25:40.

8. Schäfer M, Browne LP, Jaggers J, et al. Abnormal left ventricular flow organization following repair of tetralogy of Fallot. *J Thorac Cardiovasc Surg*. 2020;160:1008–1015.

9. Zhao X, Hu L, Leng S, et al. Ventricular flow analysis and its association with exertional capacity in repaired tetralogy of Fallot: 4D flow cardiovascular magnetic resonance study. *J Cardiovasc Magn Reson*. 2022;24:4.

10. Jeong D, Anagnostopoulos PV, Roldan-Alzate A, et al. Ventricular kinetic energy may provide a novel noninvasive way to assess ventricular performance in patients with repaired tetralogy of Fallot. *J Thorac Cardiovasc Surg*. 2015;149:1339–1347.

11. Sjöberg P, Töger J, Hedström E, et al. Altered biventricular hemodynamic forces in patients with repaired tetralogy of Fallot and right ventricular volume overload because of pulmonary regurgitation. *Am J Physiol Heart Circ Physiol*. 2018;315:H1691–H1702.

12. Hudani A, White JA, Greenway SC, Garcia J. Whole-heart assessment of turbulent kinetic energy in the repaired tetralogy of Fallot. *Applied Sciences*. 2022;12:10946.

13. Geiger J, Markl M, Jung B, et al. 4D-MR flow analysis in patients after repair for tetralogy of Fallot. *Eur Radiol*. 2011;21:1651–1657.

14. Tsuchiya N, Nagao M, Shiina Y, et al. Circulation derived from 4D flow MRI correlates with right ventricular dysfunction in patients with tetralogy of Fallot. *Sci Rep*. 2021;11:11623.

15. Loke YH, Capuano F, Cleveland V, Mandell JG, Balaras E, Olivieri LJ. Moving beyond size: vorticity and energy loss are correlated with right ventricular dysfunction and exercise intolerance in repaired Tetralogy of Fallot. *J Cardiovasc Magn Reson*. 2021;23:98.

16. Hudani A, Ihsan Ali S, Patton D, et al. 4D-Flow MRI characterization of pulmonary flow in repaired tetralogy of Fallot. *Applied Sciences*. 2023;13:2810.

17. Elsayed A, Gilbert K, Scadeng M, Cowan BR, Pushparajah K, Young AA. Four-dimensional flow cardiovascular magnetic resonance in tetralogy of Fallot: a systematic review. *J Cardiovasc Magn Reson*. 2021;23:59.

18. Stout KK, Daniels CJ, Aboulhosn JA, et al. 2018 AHA/ACC guideline for the management of adults with congenital heart disease: a report of the American College of Cardiology/American Heart Association Task Force on Clinical Practice Guidelines. *J Am Coll Cardiol*. 2019;73(12):e81–e192.

19. Baumgartner H, De Backer J, Babu-Narayan SV, et al, ESC Scientific Document Group. 2020 ESC guidelines for the management of adult congenital heart disease. *Eur Heart J*. 2021;42:563–645.

20. Dyverfeldt P, Bissell M, Barker AJ, et al. 4D flow cardiovascular magnetic resonance consensus statement. *J Cardiovasc Magn Reson*. 2015;17:72.

21. Zhong L, Schrauben EM, Garcia J, et al. Intracardiac 4D flow MRI in congenital heart disease: recommendations on behalf of the ISMRM flow and motion study group. *J Magn Reson Imaging*. 2019;50:677–681.

22. Alabed S, Maiter A, Salehi M, et al. Quality of reporting in AI cardiac MRI segmentation studies - a systematic review and recommendations for future studies. *Front Cardiovasc Med*. 2022;9:956811.

23. Zhao X, Tan RS, Garg P, et al. Age- and sex-specific reference values of biventricular flow components and kinetic energy by 4D flow cardiovascular magnetic resonance in healthy subjects. *J Cardiovasc Magn Reson*. 2023;25:50.

24. Spiewak M, Małek ŁA, Petryka J, et al. Repaired tetralogy of Fallot: ratio of right ventricular volume to left ventricular volume as a marker of right ventricular dilatation. *Radiology*. 2012;265:78–86.

25. Reddy ST, Shah M, Doyle M, et al. Evaluation of cardiac valvular regurgitant lesions by cardiac MRI sequences: comparison of a four-valve semi-quantitative versus quantitative approach. *J Heart Valve Dis*. 2013;22:491–499.

26. Leng S, Jiang M, Zhao XD, et al. Three-dimensional tricuspid annular motion analysis from cardiac magnetic resonance feature-tracking. *Ann Biomed Eng*. 2016;44:3522–3538.

27. Leng S, Dong Y, Wu Y, et al. Impaired CMR-derived rapid semi-automated right atrial longitudinal strain is associated with decompensated hemodynamics in pulmonary arterial hypertension. *Circ Cardiovasc Imaging*. 2019;12:e008582.

28. Zhao X, Tan RS, Garg P, et al. Impact of age, sex and ethnicity on intra-cardiac flow components and left ventricular kinetic energy derived from 4D flow CMR. *Int J Cardiol*. 2021;336:105–112.

29. Zhao X, Leng S, Tan RS, et al. Right ventricular energetic biomarkers from 4D Flow CMR are associated with exertional capacity in pulmonary arterial hypertension. *J Cardiovasc Magn Reson*. 2022;24:61.

30. Sjöberg P, Bidhult S, Bock J, et al. Disturbed left and right ventricular kinetic energy in patients with repaired tetralogy of Fallot: pathophysiological insights using 4D-flow MRI. *Eur Radiol*. 2018;28:4066–4076.

31. Bove AA, Santamore WP. Ventricular interdependence. *Prog Cardiovasc Dis*. 1981;23:365–388.

32. Stephensen S, Steding-Ehrenborg K, Munkhammar P, Heiberg E, Arheden H, Carlsson M. The relationship between longitudinal, lateral, and septal contribution to stroke volume in patients with pulmonary regurgitation and healthy volunteers. *Am J Physiol Heart Circ Physiol*. 2014;306:H895–H903.

33. Apitz C, Latus H, Binder W, et al. Impact of restrictive physiology on intrinsic diastolic right ventricular function and lusitropy in children and adolescents after repair of tetralogy of Fallot. *Heart*. 2010;96:1837–1841.

34. Lee W, Yoo SJ, Roche SL, et al. Determinants and functional impact of restrictive physiology after repair of tetralogy of Fallot: new insights from magnetic resonance imaging. *Int J Cardiol*. 2013;167:1347–1353.

35. Carvalho JS, Shinebourne EA, Busst C, Rigby ML, Redington AN. Exercise capacity after complete repair of tetralogy of Fallot: deleterious effects of residual pulmonary regurgitation. *Br Heart J*. 1992;67:470–473.

36. Arvidsson PM, Töger J, Heiberg E, Carlsson M, Arheden H. Quantification of left and right atrial kinetic energy using four-dimensional intracardiac magnetic resonance imaging flow measurements. *J Appl Physiol Bethesda Md. 1985*. 2013;114:1472–1481.

37. Carlsson M, Heiberg E, Toger J, Arheden H. Quantification of left and right ventricular kinetic energy using four-dimensional intracardiac magnetic resonance imaging flow measurements. *Am J Physiol Heart Circ Physiol*. 2012;302:H893–H900.

38. Alipour Symakani RS, van Genuchten WJ, Zandbergen LM, et al. The right ventricle in tetralogy of Fallot: adaptation to sequential loading. *Front Pediatr*. 2023;11:1098248.

39. François CJ, Srinivasan S, Schiebler ML, et al. 4D cardiovascular magnetic resonance velocity mapping of alterations of right heart flow patterns and main pulmonary artery hemodynamics in tetralogy of Fallot. *J Cardiovasc Magn Reson*. 2012;14:16.

40. Regen DM. Calculation of left ventricular wall stress. *Circ Res*. 1990;67:245–252.

41. Geva T, Sandweiss BM, Gauvreau K, Lock JE, Powell AJ. Factors associated with impaired clinical status in long-term survivors of tetralogy of Fallot repair evaluated by magnetic resonance imaging. *J Am Coll Cardiol*. 2004;43:1068–1074.

42. Davlouros PA, Kilner PJ, Hornung TS, et al. Right ventricular function in adults with repaired tetralogy of Fallot assessed with cardiovascular magnetic resonance imaging: detrimental role of right ventricular outflow aneurysms or akinesia and adverse right-to-left ventricular interaction. *J Am Coll Cardiol*. 2002;40:2044–2052.

43. Varga-Szemes A, Halfmann M, Schoepf UJ, et al. Highly accelerated compressed-sensing 4D flow for intracardiac flow assessment. *J Magn Reson Imaging*. 2023;58:496–507.

44. Yoon S, Nakamori S, Amyar A, et al. Accelerated cardiac MRI cine with use of resolution enhancement generative adversarial inline neural network. *Radiology*. 2023;307:e222878.

45. Jacobs KG, Chan FP, Cheng JY, Vasanawala SS, Maskatia SA. 4D flow vs. 2D cardiac MRI for the evaluation of pulmonary regurgitation and ventricular volume in repaired tetralogy of Fallot: a retrospective case control study. *Int J Cardiovasc Imaging*. 2020;36:657–669.

46. Isorni MA, Martins D, Ben Moussa N, et al. 4D flow MRI versus conventional 2D for measuring pulmonary flow after tetralogy of Fallot repair. *Int J Cardiol*. 2020;300:132–136.

47. Van den Eynde J, Derdeyn E, Schuermans A, et al. End-diastolic forward flow and restrictive physiology in repaired tetralogy of Fallot: a systematic review and meta-analysis. *J Am Heart Assoc*. 2022;11:e024036.

KEY WORDS 4D flow CMR, flow component, kinetic energy, repaired tetralogy of Fallot, right ventricular restrictive physiology

APPENDIX For an expanded Methods section and supplemental tables, please see the online version of this paper.